Catena 180 (2019) 203–211

Contents lists available at ScienceDirect

Catena

journal homepage: www.elsevier.com/locate/catena

Formation of soil phosphorus fractions along a climate and vegetation gradient in the Coastal Cordillera of Chile

Emanuel Brucker, Marie Spohn*

Department of Soil Biogeochemistry, Soil Ecology, Bayreuth Center of Ecology and Environmental Research (BayCEER), University of Bayreuth, Dr.-Hans-Frisch-Straße 1-3, 95448 Bayreuth, Germany

ARTICLE INFO

Keywords:
Nutrients
Climate sequence
Apatite weathering
Biogenic weathering
Soil turnover time

ABSTRACT

Despite the importance of phosphorus (P) for ecosystems, the effect of climate and vegetation on the formation of P fractions is not well understood. Therefore, we explored the formation of soil P fractions along a climosequence covering an arid, semi-arid, mediterranean and humid site in the Coastal Cordillera of Chile. We determined Hedley P fractions (water extractable P, labile P, secondary mineral P, apatite P and residual P) as well as total organic P (TOP) in two soils on each of the four study sites. We calculated apatite dissolution rates based on the soil production rate and the soil P fractions, which has never been done before, according to our knowledge. Apatite P was the dominant P fraction in the soils at the arid and the semiarid site, and it decreased from the arid to the humid site by 96%. Residual P and secondary mineral P dominated at the humid site. The increase in plant available P along the climosequence went along with an increase in TOP. Apatite was strongly positively correlated with soil pH across all soils. The apatite dissolution rate increased with mean annual precipitation from 0 to 34 mg P m^{-2} yr^{-1}, leading to an increase in plant available P (sum of water extractable P and labile P) along the climosequence from the arid to the humid site. In conclusion, our study shows that the extent to which apatite in soil is dissolved, and the apatite dissolution rate strongly increase with precipitation, leading to an increase in the concentrations of secondary soil P fractions (secondary mineral P, labile P and TOP) along the climosequence.

1. Introduction

The formation of soil phosphorus (P) fractions plays an important role in ecosystem development because it largely affects the availability of P for biota (Walker and Syers, 1976; Wardle et al., 2004). While it has been studied intensively how soil P fractions are influenced by soil age, little is known about the effect of precipitation, vegetation and soil production rate on the formation of soil P fractions. The effect of precipitation of soil P fractions might be especially important because of predicted future changes in precipitation in many parts of the world (Trenberth et al., 2014).

The formation of P fractions during pedogenesis is described by the Walker and Syers model (Walker and Syers, 1976). At initial stages of soil development, the total P (TP) pool is dominated by P present in the form of primary minerals, mainly apatites. During soil development, the apatite concentration decreases due to apatite dissolution (apatite weathering). The released inorganic P forms secondary P fractions such as secondary mineral P, which is P sorbed to (hydr-)oxides of iron (Fe), aluminum (Al) and manganese (Mn). In addition, a part of the released inorganic P is taken up by biota that transform inorganic P into organic P, which dominates the soil TP pool at later stages of soil development. Chronosequence studies largely confirmed the Walker and Syers model for different climate zones (Lajtha and Schlesinger, 1988; Crews et al., 1995; Richardson et al., 2004; Selmants and Hart, 2010; Chen et al., 2015).

Chemical and physical weathering rates of minerals such as apatite are influenced by precipitation (West et al., 2005; Maher, 2010). Furthermore, plants and microorganisms contribute to weathering of apatite in several ways: (1) They take up phosphate, and thus remove it from the soil solution, which can lead to undersaturation of the solution, and thus increases apatite weathering, (2) they release siderophores and other chelators that increase the solubility of P, and (3) they work as a source of protons by releasing acids and protons. Finally, (4) they become a source of carbonic acid when being decomposed (Hinsinger, 2001; Jones and Oburger, 2011; Uroz et al., 2009). The input of protons leads to apatite dissolution because apatite dissolution is a pH-dependent, proton-consuming process (Guidry and Mackenzie, 2003). Therefore, it seems reasonable to assume that apatite dissolution

* Corresponding author.
E-mail address: marie.spohn@uni-bayreuth.de (M. Spohn).

https://doi.org/10.1016/j.catena.2019.04.022
Received 9 November 2018; Received in revised form 1 April 2019; Accepted 19 April 2019
Available online 02 May 2019
0341-8162/

and the formation of secondary P fractions are controlled by precipitation and vegetation.

The few existing climosequence studies that investigated P fractions revealed decreasing amounts of apatite P and increasing amounts of secondary mineral P with increasing precipitation (Ippolito et al., 2010; Emadi et al., 2012; Feng et al., 2016). Amounts of apatite P decreased along a precipitation gradient ranging from 850 to 5000 mm yr^{-1} in Maui, Hawaii, while organic P increased (Miller et al., 2001). Similarly, the amount of apatite P decreased by 60% in A horizons along a precipitation gradient ranging from 550 to 1250 mm precipitation yr^{-1} in northern Iran (Emadi et al., 2012). Total organic P (TOP) was positively correlated with mean annual precipitation (MAP) in a precipitation gradient ranging from 34 to 436 mm yr^{-1} in grasslands in northern China (Feng et al., 2016).

While many studies on soil P dynamics take into account the age of soils, only very few studies on soil P consider that soils are continuously produced by the weathering of parent material, and at the same time, are continuously eroded, leading to a constant turnover of soil. The soil residence time, i.e., the time between parent material is turned into soil (soil production) and soil denudation, determines the time during which apatite can weather in soil (Porder et al., 2007; Buendia et al., 2010). If dissolution processes take longer than the residence time, only a small part of the apatite present in the parent material dissolves, and hence the concentrations of secondary P fractions are low (Porder et al., 2007; Buendia et al., 2010). Yet, except for a few modeling studies (Porder et al., 2007; Buendia et al., 2010; Spohn and Sierra, 2018), the dynamic of soil production and erosion has not been taken into account in studies exploring the formation of soil P fractions.

We investigated the effect of precipitation and soil production rate on the formation of soil P fractions. We hypothesized that i) concentrations of apatite P decrease along the climosequence from the arid to the humid site; ii) the soil apatite dissolution rate increases along the climosequence from the arid to the humid site; and iii) TOP concentrations increase along the climosequence from the arid to the humid site. In order to test these hypotheses, we studied soils along a climate and vegetation gradient ranging from arid to humid climate in the Coastal Cordillera of Chile. The sites were chosen because they differ in precipitation and have a similar lithology given the large maximum geographical distance of 1300 km. The investigated soils developed on plutonic rocks of similar granitoid lithology. The sites were free of glaciation during the last ice age and have not received inputs of volcanic material. All of them are situated in national parks or nature reserves, which minimizes anthropogenic influences. The sites haven been described elsewhere in detail (Oeser et al., 2018; Bernhard et al., 2018). Based on the description of a short *catena* on each site (Oeser et al., 2018; Bernhard et al., 2018), we chose to study two representative profiles at each site.

2. Materials and methods

2.1. Study sites

The four study sites Pan de Azúcar, Santa Gracia, La Campana and Nahuelbuta are located between 26° S and 38° S in the Coastal Cordillera of Chile. They form a precipitation sequence covering arid, semi-arid, mediterranean and humid climate with rainfall increasing from 10 to 1084 mm yr^{-1} (Table 1). The investigated soils developed on plutonic rocks of similar granitoid lithology. All sites were free of glaciation during the last glacial maximum (~19,000–23,000 yr ago, Hulton et al., 2002) and have not received inputs of volcanic material (Oeser et al., 2018). Based on the description of a short *catena* on each site (Oeser et al., 2018; Bernhard et al., 2018), we chose to study two representative profiles at each site, one on a north-facing slope and one on a south-facing slope.

The arid site Pan de Azúcar is located in the southern range of the Atacama Desert, and is part of the national park Pan de Azúcar. The two

Table 1
Characteristics of the four sites and the eight soils in the Costal Cordillera in Chile. Denudation rates were taken from Schaller et al. (2018). The soils were classified according to the World Reference Base for Soil Resources (WRB).

Site	MAT [°C]	MAP [mm a^{-1}]	Climate classification	Aspect	Southern latitude	Western longitude	Elevation [m.a.s.l.]	Soil type	Denudation rate [t km^{-2} yr^{-1}]
Pan de Azúcar	18.1	10	Arid	North-facing	26.1093	70.5491	343	Regosol	8.2 ± 0.5
				South-facing	26.1102	70.5493	330	Regosol	11.0 ± 0.7
Santa Gracia	16.1	87	Arid/semiarid	North-facing	29.7612	71.1656	690	Cambisol	15.9 ± 0.9
				South-facing	29.7574	71.1664	682	Cambisol	22.4 ± 1.5
La Campana	14.9	436	Mediterranean	North-facing	32.9573	71.0643	743	Cambisol	69.2 ± 4.6
				South-facing	32.9559	71.0635	730	Cambisol	53.7 ± 3.4
Nahuelbuta	14.1	1084	Humid	North-facing	37.809	73.0138	1219	Umbric Podzol	17.7 ± 1.1
				South-facing	37.8077	73.0135	1239	Orthodystric Umbrisol	47.5 ± 3.0

soils on the north- and on the south-facing slope were classified as Regosols with a shallow A horizon over a B horizon of 0.20 m maximum thickness followed by saprolite (Cw horizon) (Bernhard et al., 2018). The vegetation is very sparse. The soils are covered with a thin soil crust formed by algae (Baumann et al., 2018). The arid to semi-arid site Santa Gracia is located in a private reserve. In order to distinguish it from the previous site we will call it semiarid in the following. The soil on the north-facing slope at this site was classified as a Leptosol with cambic properties, and the soil on the south-facing slope as a Cambisol. The Ah horizons are 0.10 m thick and the Bw horizons reach down to 0.25–0.3 m soil depth. The vegetation is formed by shrubs and cacti, while herbaceous plants are sparse. The mediterranean site is located in the national park La Campana. The soils were classified as Cambisols. The organic horizons are approximately 5 cm thick, the Ah horizons reach 0.4 m in thickness and are followed by Bw horizons that extend down to 0.6 m. The site hosts a sclerophyll forest. The humid site is located in the national park Nahuelbuta. The soils were classified as an Umbric Podzol (north-facing slope) and an Orthodystric Umbrisol (south-facing slope). The Ah horizons measure 0.35–0.50 m and are overlain by organic horizons of up to 5.5 cm thickness. The Bw horizons reach down to 0.80 m total soil depth. The main tree species are southern beech (*Nothofagus*) and monkey puzzle trees (*Araucaria*) with an understory of shrubs, bamboo and grasses. Further details about climate, parent material, soils and vegetation are given in Oeser et al. (2018) and Bernhard et al. (2018).

2.2. Sampling and sample preparation

Samples were collected using a small shovel and a trowel from the following depth increments 0–0.05, 0.05–0.1, 0.1–0.2, 0.2–0.4, 0.4–0.6, 0.6–0.8, 0.8–1.0, 1.0–1.2, 1.2–1.4, 1.4–1.6, 1.6–1.8 and 1.8–2.0 m until the Cw horizon. Bulk density was determined gravimetrically from volumetric samples (100 cm^3 steel cylinders). The soil profiles were prepared directly before sampling, which allowed us to collect fresh soil material. The samples were sieved (< 2 mm) in field moist conditions and roots were gently removed. Samples were milled, sieved and oven-dried (105 °C) before the X-Ray Fluorescence (XRF) measurements were performed to determine TP. Other soil chemical analyses were conducted with sieved (< 2 mm) and air-dried (at 20 °C) samples, unless specified otherwise.

2.3. Soil chemical analyses

To determine soil P fractions, a modified version of the Hedley fractionation (Hedley et al., 1982) was used following Tiessen and Moir (1993). For this purpose, 0.5 g of ground soil and 30 ml of the respective reaction reagents were used. Samples were sequentially extracted in H_2O (water-extractable P), 0.5 M $NaHCO_3$ (labile P), 0.1 M NaOH (secondary mineral P, Fe- and Al-associated P) and 1 M HCl (apatite P) during 16 h on a horizontal shaker. Subsequently, the sample was centrifuged (4100 × *g* for 15 min). Total P (organic and inorganic) concentrations in the $NaHCO_3$-, NaOH- and HCl-extracts were determined using ICP-OES (Vista-Pro radial, Varian). Inorganic phosphate concentrations in the water extracts were determined spectrophotometrically by the molybdenum-blue method (Murphy and Riley, 1962) and measured on a platereader (M200 Pro, Tecan Group Ltd., Switzerland).

Total P was determined using a XRF spectrometer (PANalytical AXIOS advanced, Malvern Panalytical, The Netherlands) at the German Research Centre for Geosciences. For this purpose, beads consisting of 1 g sample material, 6 g dilithiumtetraborate and up to 1 g ammonium nitrate were prepared in a heating system. All values were corrected for loss by ignition and were expressed on a volatile free basis.

The determination of TOP followed the description of Saunders and Williams (1955) modified by Walker and Adams (1958). Briefly, the TOP concentration was determined as the difference of P extracted from a sample ignited at 550 °C in a muffle furnace and a non-ignited sample. Both samples were extracted for 16 h in 0.5 M H_2SO_4 on a horizontal shaker and subsequently centrifuged at 1500 × *g* for 15 min. The concentrations of inorganic P in the 0.5 M H_2SO_4 extracts were determined according to the molybdenum-blue method (Murphy and Riley, 1962) and measured with a spectrophotometer (UV-1800, Shimadzu Corp., Japan). The pH was measured in 0.01 M $CaCl_2$ with a soil:solution ratio of 1:2.5 using a pH meter (pH 340, WTW GmbH, Weilheim, Germany) with a Sentix 81 electrode.

2.4. Calculations

The dissolution rate of apatite and the rate at which TP is denudated were calculated based on the P fractions and the denudation rate (Table 1) determined by Schaller et al. (2018) using ^{10}Be concentrations. Denudation is the sum of erosion and leaching. It should be noted that we use the term rate here when refering to a certain amount per area per time as it is common practice in empirical studies on weathering (Hartmann et al., 2014; Zhou et al., 2018), while in modeling studies this is refered to as a flux (Buendia et al., 2010; Spohn and Sierra, 2018). First, soil P stocks were calculated based on TP concentrations, bulk density and the thickness of the respective depth increment, up to a soil depth of 1 m. If samples were not taken down to 1 m depth, bulk density and TP concentration in the remaining soil up to 1 m were assumed to equal those of the lowest measured depth increment. Second, the total soil mass per m^2 down to 1 m was calculated based on the bulk densities of the different depth increments. Denudation rates determined by Schaller et al. (2018) were used to calculate the mean residence time of the upper meter of soil, based on the assumption that the soil production rate equals the denudation rate (steady-state). This steady-state assumption is commonly made in studies on soil denudation (Riebe et al., 2003; Dixon et al., 2009).

$$\textit{Residence time of 1 m of soil (yr)} = \frac{\textit{Soil mass in the upper 1 m (kg m}^{-2}\textit{)}}{\textit{Denudation rate (kg m}^{-2}\textit{ yr}^{-1}\textit{)}} \quad (1)$$

The TP denudation rate, which equals the rate with which P is lifted from the saprolite into the soil, was calculated as follows:

$$\textit{TP denudation rate (mg P m}^{-2}\textit{ yr}^{-1}\textit{)} = \frac{\textit{TP stock in the upper 1 m (mg P m}^{-2}\textit{)}}{\textit{Residence time of 1 m of soil (yr)}} \quad (2)$$

The rate of apatite dissolution (apatite weathering) was calculated based on the proportion of apatite P of the TP stock in the upper 0.05 m of the soils, assuming that this is the maximum amount of apatite P that remains in the soils non-dissolved until the soil erodes.

$$\textit{Apatite dissolution rate (mg P m}^{-2}\textit{yr}^{-1}\textit{)} = \textit{TP denudation rate (mg P m}^{-2}\textit{ yr}^{-1}\textit{)} \times \left(1 - \left(\frac{\textit{Apatite P}_{\textit{Upper 0.05 m}}}{\textit{Total P}_{\textit{Upper 0.05 m}}}\right)\right) \quad (3)$$

3. Results

The TP stocks in the first meter of the soils ranged between 0.5 and 1.1 kg m^{-2}, and showed no clear trend along the climosequence (Table 2). The size of the five P fractions differed among the four study sites. While apatite P was the dominant P fraction at the arid and the semiarid site, residual P and secondary mineral P dominated at the mediterranean and the humid site (Fig. 1, Supplement A). The apatite P fraction strongly decreased along the climosequence from the arid to the humid site, and the decrease amounted to 95–96%, 88–97%, and 83% of the soil apatite P concentrations at the arid site in the depth increments 0–0.05, 0.20–0.40, and 0.60–0.80 m, respectively (Fig. 1).

Table 2
Total P (TP) stocks in the upper first meter of the soils, TP denudation rates and the rates of apatite dissolution in two soils at each of the four sites (one at a North- and one at a South-facing slope).

	Arid site		Semiarid site		Mediterranean site		Humid site	
	North-facing	South-facing	North-facing	South-facing	North-facing	South-facing	North-facing	South-facing
TP stock (in upper 1 m) [kg m^{-2}]	0.7	1.1	0.8	0.7	0.8	0.6	0.5	0.7
TP denudation rate [mg m^{-2} yr^{-1}]	4.3 ± 0.3	7.5 ± 0.4	7.8 ± 0.4	10.2 ± 0.7	34.2 ± 2.3	25.9 ± 1.6	7.6 ± 0.5	35.6 ± 2.3
Apatite dissolution rate [mg P m^{-2} yr^{-1}]	0.0	0.6 ± 0.0	2.9 ± 0.2	4.4 ± 0.3	23.4 ± 1.6	20.2 ± 1.3	7.3 ± 0.4	34.4 ± 2.2

This trend was observed for the absolute apatite P concentrations as well as for the proportion of apatite P in relation to TP. The apatite P fraction was positively correlated with soil pH across the climosequence ($r^2 = 0.91$, $p < 0.001$ and $r^2 = 0.86$, $p < 0.001$) in the depth increments 0–0.05 m and 0.20–0.40 m, respectively (Fig. 2a). The apatite P fraction decreased with increasing precipitation from the arid to the humid site (Fig. 3a). An increase in precipitation by 77 mm from the arid to the semiarid site went along with a decrease in apatite P by 57–63% in the first 0.05 m of the soils. In the same depth increment, the apatite P fraction decreased from the mediterranean to the humid site by 65–81%, although the increase in precipitation (648 mm) was eight times larger compared to the increase in precipitation from the arid to the semiarid site (Fig. 3a).

Rates of P denudation ranged between 4.3 ± 0.3 and 35.6 ± 2.3 mg P m^{-2} yr^{-1} and were highest at the mediterranean site (on both slopes) and on the south-facing slope at the humid site (Table 2). Rates of apatite dissolution increased along the climosequence from 0.0 in the soils on the north-facing slope at the arid site to up to 34.4 mg P m^{-2} yr^{-1} in the soil on the south-facing slope at the humid site (Table 2). The apatite dissolution rate increased strongly with precipitation, and only the soil on the north-facing slope at the humid site showed a relatively low apatite dissolution rate despite high

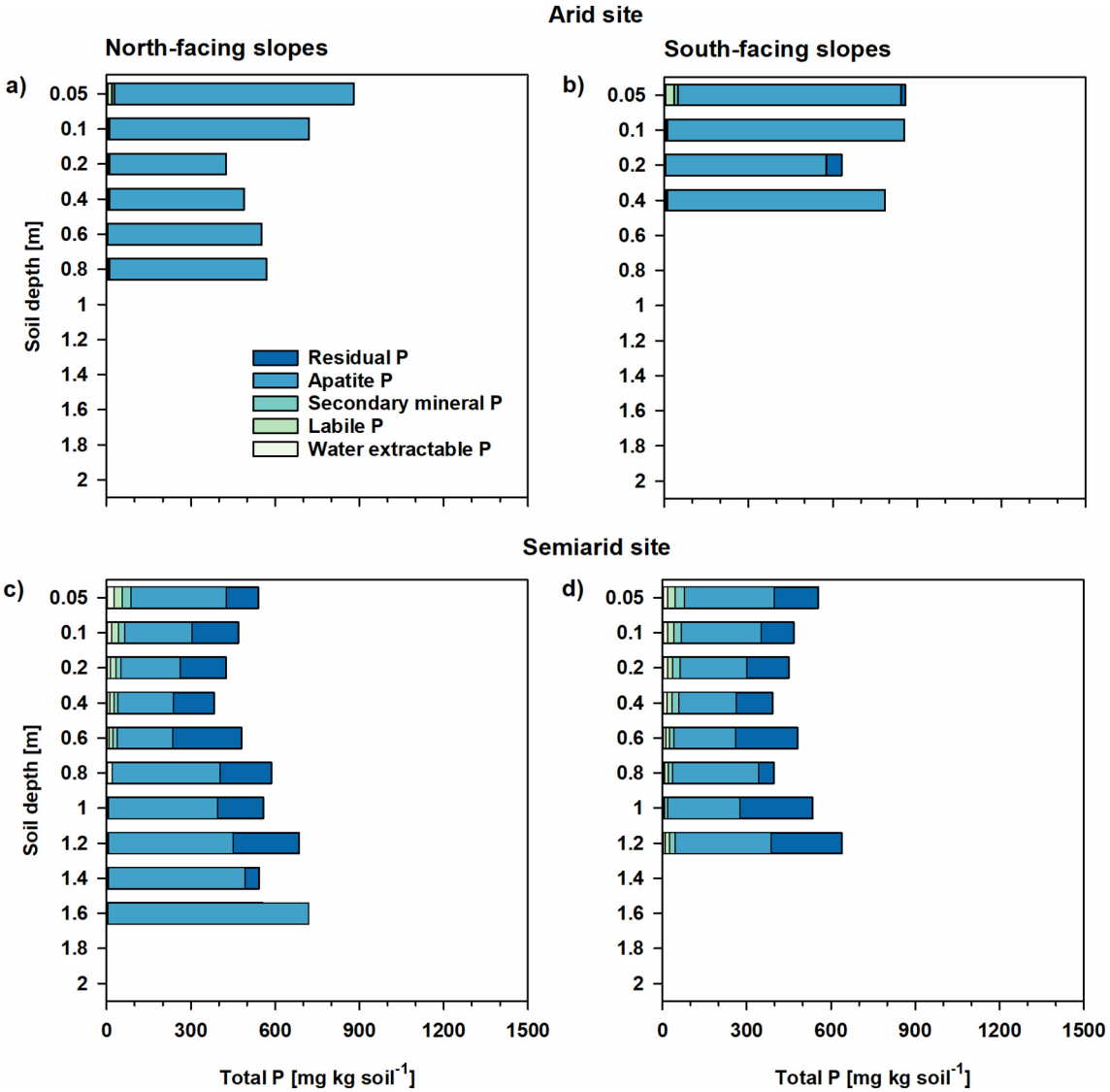

Fig. 1. Phosphorus (P) concentrations of five fractions in soils at the arid (a and b), the semiarid (c and d), the mediterranean (e and f) and the humid site (g and h) on the north-facing slope (a, c, e, g) and the south-facing slope (b, d, f, h) at each of the four sites.

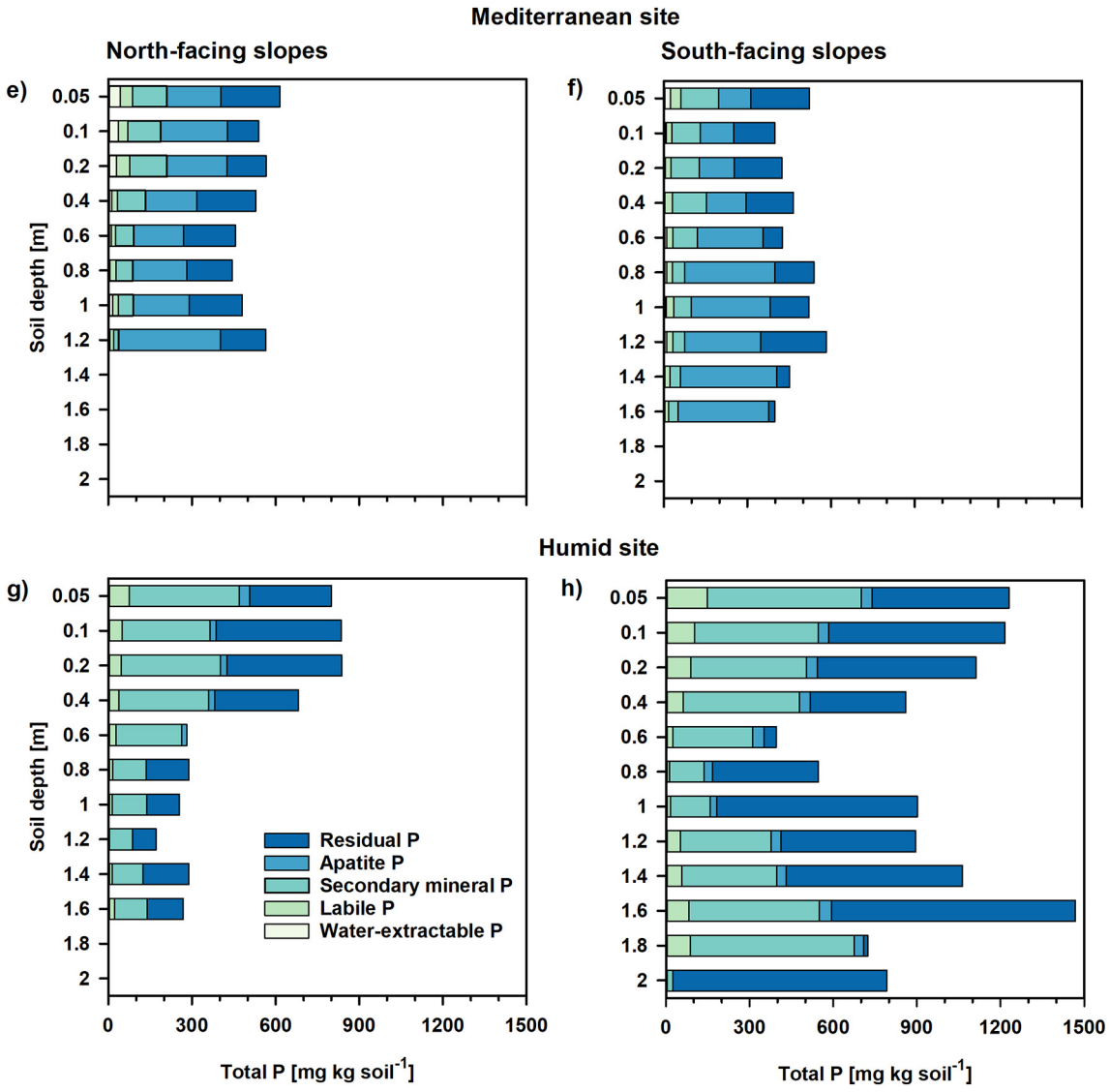

Fig. 1. (*continued*)

precipitation (Fig. 3b).

The sum of water- and $NaHCO_3$-extractable P increased from the arid to the humid site in the depth increment 0–0.05 m. The same was observed in the depth increment 0.20–0.40 m but with 28–70% lower concentrations compared to the depth increment 0–0.05 m (Fig. 1).

Secondary mineral P increased from 1% of TP at the arid site to up to 50% of TP at the humid site in the first 0.40 m of the soils (Fig. 1). Secondary mineral P decreased with increasing soil depth in almost all soils, except for the ones at the humid site (Fig. 1). Secondary mineral P in the depth increments 0–0.05 m and 0.20–0.40 m was negatively correlated with pH ($r^2 = 0.77$, $p < 0.01$ and $r^2 = 0.61$, $p < 0.05$, respectively; Fig. 2b) and positively correlated with the sum of oxalate extractable Fe and Al ($r^2 = 0.84$, $p < 0.05$) in the depth increment 0.60–0.80 m (data not shown).

Residual P strongly increased along the climosequence from the arid to the humid site. In the depth increment 0.20–0.40 m, the residual P concentration increased along the sequence from the arid to the humid site by 80–106% compared to the concentrations in the soils at the arid site (Fig. 1).

TOP increased along the climosequence from the arid to the humid site both in absolute terms (Fig. 4) and also relative to the TP concentrations. It increased from 6 to 18% of TP at the arid site to 44–51% of TP at the humid site, in the first 0.05 m of the soils. With increasing soil depth, TOP decreased, and this decrease was largest at the humid site.

4. Discussion

4.1. Apatite

We found that the apatite P concentration decreased along the climosequence with increasing MAP. In the low precipitation range, a small increase in precipitation went along with a large decrease in the apatite concentration (Fig. 3a). Our finding that the apatite concentration did not decrease linearly with precipitation, but decreased more strongly with increasing precipitation in the low precipitation range than in the high precipitation range, is in agreement with similar observations made along a rainfall gradient in Hawaii (Vitousek and Chadwick, 2013). The relatively large soil chemical transitions at the low precipitation range of climosequences have been described as a pedogenic threshold. Pedogenic thresholds occur where soil properties change abruptly or nonlinearly with a small increment in environmental forcing (Chadwick and Chorover, 2001). The pedogenic threshold might be caused by higher plants (Vitousek and Chadwick, 2013) that are absent at the arid site but present at the semi-arid site and very likely massively enhance apatite dissolution due to root

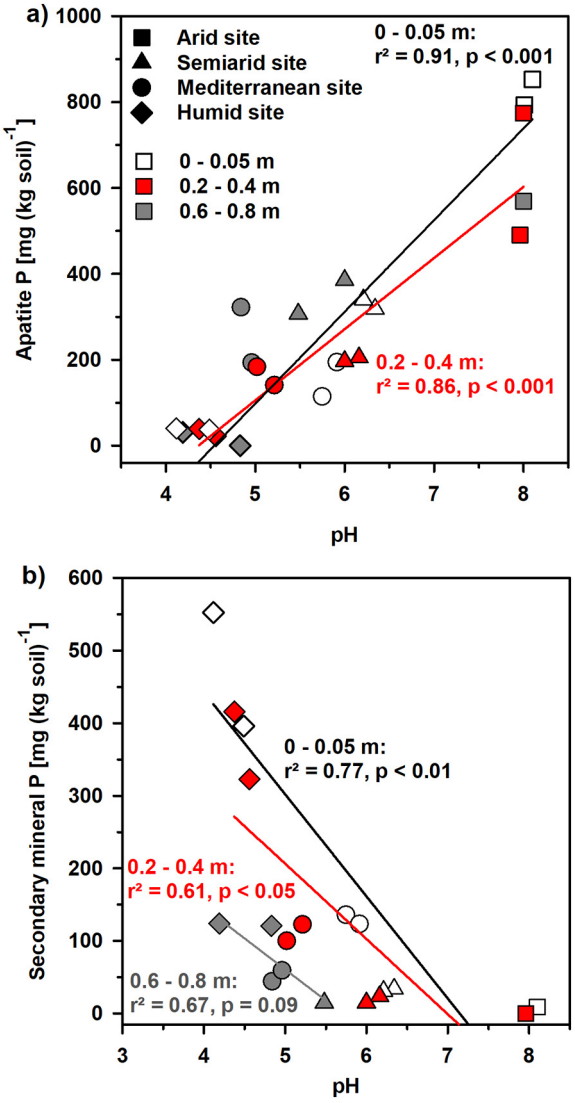

Fig. 2. Relationship of apatite P and pH (a) and secondary mineral P and pH (b) in soils at the arid, semiarid, mediterranean and humid site. Data from the three soil depth increments 0–0.05 m (white), 0.20–0.40 m (red) and 0.60–0.80 m (dark-grey) are shown, the r^2 value gives the Pearson correlation coefficient calculated separately for each soil depth increment. (For interpretation of the references to colour in this figure legend, the reader is referred to the web version of this article.)

respiration, the release of protons as well as organic acids, and the removal of phosphate from the soil solution (Hinsinger, 2001). The pedogenic threshold might also be caused by soil pH, which decreases along the gradient form the arid to the humid site (Bernhard et al., 2018). This is supported by the observation that the concentration of apatite was linearly related with soil pH (Fig. 2a). Higher soil acidity favours the dissolution of apatite because apatite dissolution is a pH-dependent, proton-consuming process (Hinsinger, 2001). The finding that the apatite P fraction was the largest P fraction at all sites, except for the humid site, is in accordance with a recent study on P fractions in biocrusts that investigated the P fractions in the upper mm of the soils at the same four sites (Baumann et al., 2018). Taken together, our findings confirm the first hypothesis that the concentration of apatite in the soils decreases along the climosequence, which can be related to an increase in soil acidity from the arid to the humid site.

4.2. Apatite dissolution rates

The apatite dissolution rate increased with MAP (Fig. 3b; Table 2) and was highest in the soil on the south-facing slope at the humid site (Table 2). Besides depending on chemical conditions (such as soil acidity, see above), the amount of P released from apatite per area per time (apatite dissolution rate) depends on the apatite content of the saprolite, the soil production rate and the soil residence time because they determine the amount of apatite input to the soil and the time during which apatite can weather (Porder et al., 2007). In the soils under study, the soil production rates and the apatite contents of the saprolite were large enough to lead to a considerable input of apatite to the soils, and the soil residence times were large enough to allow for dissolution of apatite, except for the arid site (north-facing slope), where low precipitation and high pH values did not favor apatite dissolution. The findings confirm our second hypothesis that the apatite dissolution rate increases along the climosequence from arid to humid climate.

The apatite dissolution rates found for the semiarid and mediterranean site were similar to the ones calculated by Hartmann et al. (2014) as a global mean for acid plutonic and neutral plutonic rock (10.92 and 6.63 mg P m^{-2} yr^{-1}). Yet, the rates at the arid and humid site (south-facing slope) differed from the global means, highlighting the importance of climate for apatite weathering. The apatite dissolution rates determined here are considerably lower than apatite dissolution rates calculated for young soils based on chronosequences in glacier moraines that amounted to several hundreds of mg P m^{-2} yr^{-1} (Föllmi et al., 2009; Zhou et al., 2018). This is because weathering rates tend to be very high during early stages of soil development. However, the rates are in agreement with apatite dissolution rates at sites of chronosequences that are > 10,000 years old (Walker and Syers, 1976; Föllmi et al., 2009). The agreement of the apatite weathering rates calculated here based on denudation rates and P fractions and the rates determined in previous studies by various other methods for mature soils confirms that our approach gives reasonable estimates of apatite dissolution rates.

This is the first study, to our knowledge, that calculates apatite dissolution rates based on soil P fractions and soil production rates. The large advantage of this approach is that the dissolution rate is calculated based on data gained from the soil profiles, without measurements of stream-water or performance of lab incubations. Yet, as any method this approach is also based on some assumptions. The most important assumptions are i) that all soil P is derived from the parent material and ii) that there is no net transport of P in the soil profile. The first assumption can relatively confidently been made in the present study since atmospheric P deposition is predicted to be very small at the Chilean sites, ranging between 0.05 and 0.2 mg P m^{-2} yr^{-1} (Penuelas et al., 2013). Thus, at our study sites, atmospheric inputs should hardly contribute to the P budget. In fact, the inputs might be lower than the ones estimated by Penuelas et al. (2013) because the study sites are located in remote areas far away from cities. The second assumption is more difficult to evaluate since data on translocation of P in soil profiles is scarce. Since the precipitation rates were low at most sites, and did not exceed 1100 mm yr^{-1} at the humid site, it seems likely that leaching of P in soils is negligible. However, one of the soils at the humid site was a Podzol (Bernhard et al., 2018), indicating that P might have been translocated from the E horizon into the subsoil. However, we only found a small decrease in labile P in a depth of 0.05–0.1 m compared to the two soil depth increments above and below (Fig. 1). Thus, our assumption that no major net change in the P contents in the soil profile occurred seems acceptable for the soils under study. Our approach to calculate apatite dissolution rates works very likely also for other soils in areas with rather low precipitation rates, and thus low rates of P leaching and P eluviation (Selmants and Hart, 2010). Yet, it might not work at sites, where high precipitation rates lead to leaching of P (Walker and Syers, 1976; Chadwick et al., 1999). Leaching of

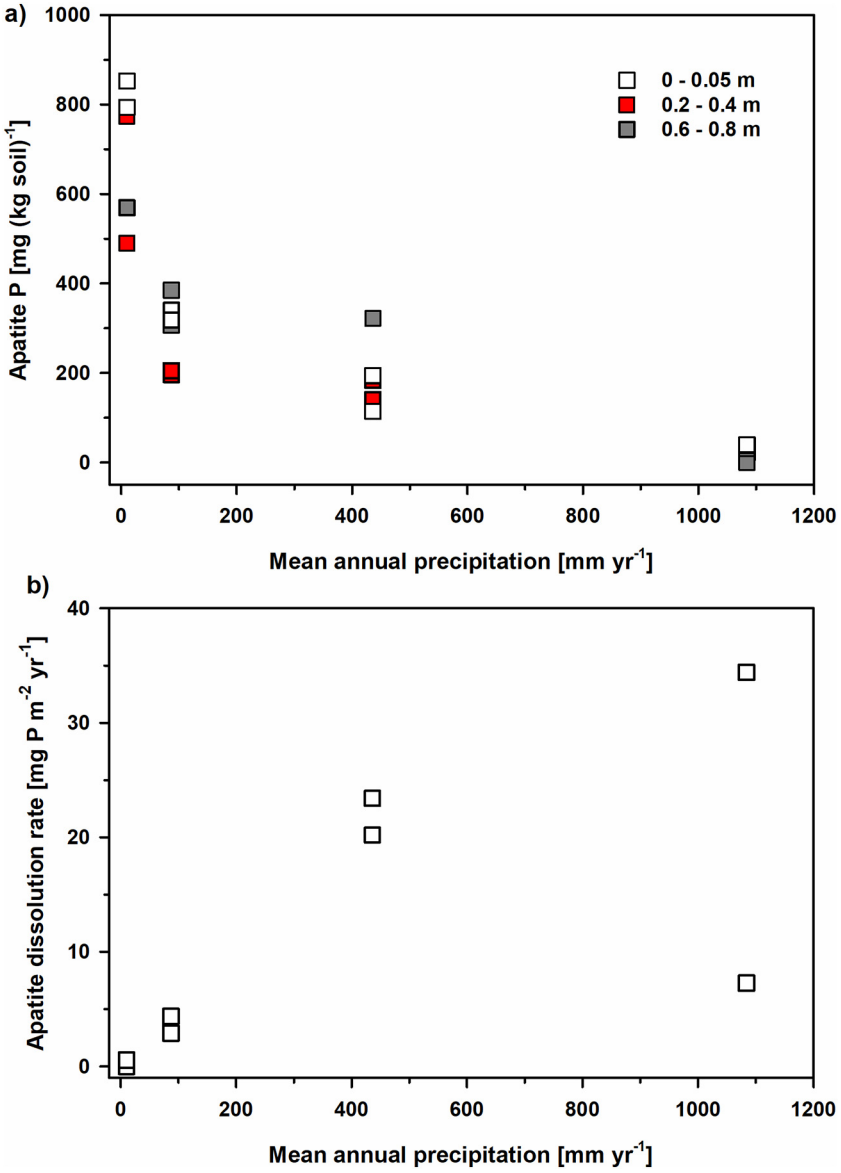

Fig. 3. Apatite P concentration (a) and apatite dissolution rate (b) as a function of mean annual precipitation across the arid, the semiarid, the mediterranean and the humid site.

secondary P fractions from the upper cm of the soils will lead to an increase in the ratio of apatite P-to-total P in the upper cm of the soils in Eq. (3) (see above), and thus to an underestimation of the apatite dissolution rate. For soils in which secondary mineral P is eluviated in the profile, one might consider calculating the ratio of apatite P-to-total P not only for the upper 0.05 m as in Eq. (3) but for the whole profile, in order to estimate the apatite dissolution rate.

4.3. Secondary forms of phosphorus

The sum of water-extractable and labile P, which represents the P fraction readily available for plant uptake, increased along the climosequence (Fig. 1). The formation of the plant available P pool depends on the apatite dissolution rate and on the amount of Al and Fe (hydro-) oxides. The latter is indicated by the correlation of secondary mineral P and the sum of oxalate extractable Fe and Al across all soils. The relatively high concentrations of bioavailable P at all sites except for the arid site (north-facing slope) indicate that P was not limiting for primary production.

It has to be taken into account that we used Hedley fractionation to gain soil P fractions. Hedley fractionation is a well-established technique that has been used in hundreds of studies in soil science (for reviews see Cross and Schlesinger, 1995; Yang and Post, 2011; Hou et al., 2018). Yet, Hedley fractionation gives operational defined pools that are not completely pure. It also needs to be taken into account that we determined total P in the fractions, which includes organic and inorganic P. However, we also determined TOP concentrations separately.

TOP concentrations increased along the climosequence from the arid to the humid site, which is likely due to (1) an increase in NPP with increasing precipitation (Werner et al., 2018) and (2) the increase in plant available P along the climosequence. The relatively large plant available P fraction allowed for high plant P uptake, while the rise in NPP along the climosequence likely led to an increase in plant litter (and thus OP) inputs to soil along the sequence. The increase in TOP in the soils along the climosequence from the arid to the humid site is in accordance with a previous study, reporting that the TOP concentration in the upper 0.10 m of the soils increased from 80 to 430 mg TOP kg^{-1} in a precipitation gradient, ranging from 34 to 436 mm yr^{-1} in grasslands in northern China (Feng et al., 2016). Our results are also in

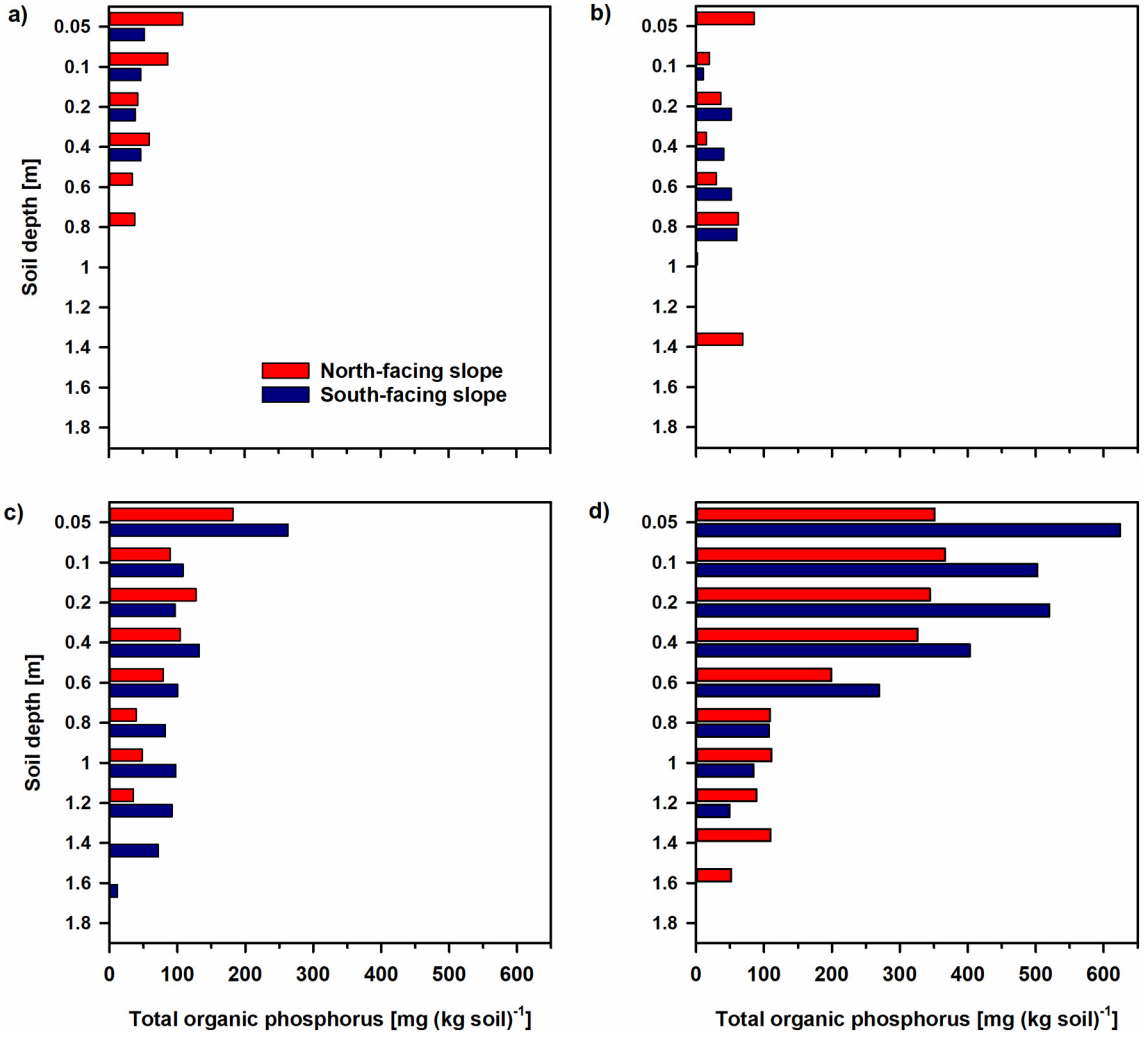

Fig. 4. Total organic P (TOP) in soils at the arid (a), the semiarid (b), the mediterranean (c) and the humid site (d) in two soils at each of the four sites.

agreement with data of a global meta-analysis, showing that TOP increases with an increase in precipitation from 0 to 1000 mm yr^{-1} (Hou et al., 2018). Taken together, our findings confirm the third hypothesis that concentrations of TOP increase along the climosequence from the arid to the humid site.

5. Conclusions

Our study shows that the extent to which apatite in soils is dissolved, strongly increases along the climosequence from the arid to the humid site, leading to an increase in the concentration of secondary soil P fractions (secondary mineral P, labile P and TOP) along the sequence with increasing precipitation. We calculated apatite dissolution rates based on the soil production rate and the soil P fractions, which has never been done before, according to our knowledge. The apatite dissolution rates increased with precipitation, highlighting the importance of climate for weathering and soil P dynamics. Our study indicates that soil production rates should be taken into account when evaluating the formation of soil P fractions.

Acknowledgements

We acknowledge support from the German Science Foundation (DFG) priority research program SPP-1803 “EarthShape: Earth Surface Shaping by Biota” (grant DFG SP 1389/5-1). We are grateful to the Chilean National Park Service (CONAF) for providing access to the sample locations and on-site support of our research. Further we would like to thank Renate Krauß for her help in laboratory work and the BayCEER Laboratory for Analytical Chemistry at the University of Bayreuth for chemical analyses.

Appendix A. Supplementary data

Supplementary data to this article can be found online at https://doi.org/10.1016/j.catena.2019.04.022.

References

Baumann, K., Jung, P., Samolov, E., Lehnert, L.W., Büdel, B., Karsten, U., Bendix, J., Achilles, S., Schermer, M., Matus, F., Oses, R., Osses, P., Morshedizad, M., Oehlschläger, C., Hu, Y., Klysubun, W., Leinweber, P., 2018. Biological soil crusts along a climatic gradient in Chile: richness and imprints of phototrophic microorganisms in phosphorus biogeochemical cycling. Soil Biol. Biochem. 127, 286–300.

Bernhard, N., Moskwa, L.M., Schmidt, K., Oeser, R.A., Aburto, F., Bader, M.Y., et al., 2018. Pedogenic and microbial response to regional climate and local topography: insights from a climate gradient (arid to humid) on granitoid parent material in Chile. Catena 170, 335–355.

Buendia, C., Kleidon, A., Porporato, A., 2010. The role of tectonic uplift, climate, and vegetation in the long-term terrestrial phosphorous cycle. Biogeosciences 7, 2025–2038.

Chadwick, O.A., Chorover, J., 2001. The chemistry of pedogenic thresholds. Geoderma 100, 321–353.

Chadwick, O.A., Derry, L.A., Vitousek, P.M., Huebert, B.J., Hedin, L.O., 1999. Changing sources of nutrients during four million years of ecosystem development. Nature 397, 491.

Chen, C.R., Hou, E.Q., Condron, L.M., Bacon, G., Esfandbod, M., Olley, J., Turner, B.L.,

2015. Soil phosphorus fractionation and nutrient dynamics along the Cooloola coastal dune chronosequence, southern Queensland, Australia. Geoderma 257, 4–13.
Crews, T.E., Kitayama, K., Fownes, J.H., Riley, R.H., Herbert, D.A., Mueller-Dombois, D., Vitousek, P.M., 1995. Changes in soil phosphorus fractions and ecosystem dynamics across a long chronosequence in Hawaii. Ecology 76, 1407–1424.
Cross, A.F., Schlesinger, W.H., 1995. A literature review and evaluation of the Hedley fractionation: applications to the biogeochemical cycle of soil phosphorus in natural ecosystems. Geoderma 64, 197–214.
Dixon, J.L., Heimsath, A.M., Amundson, R., 2009. The critical role of climate and saprolite weathering in landscape evolution. Earth Surf. Process. Landf. 34, 1507–1521.
Emadi, M., Baghernejad, M., Bahmanyar, M.A., Morovvat, A., 2012. Changes in soil inorganic phosphorous pools along a precipitation gradient in northern Iran. Int. J. For. Soil Erosion 2, 143–147.
Feng, J., Turner, B.L., Lü, X., Chen, Z., Wei, K., Tian, J., et al., 2016. Phosphorus transformations along a large-scale climosequence in arid and semiarid grasslands of northern China. Glob. Biogeochem. Cycles 30, 1264–1275.
Föllmi, K.B., Hosein, R., Arn, K., Steinmann, P., 2009. Weathering and the mobility of phosphorus in the catchments and forefields of the Rhône and Oberaar glaciers, central Switzerland: implications for the global phosphorus cycle on glacial–interglacial timescales. Geochim. Cosmochim. Acta 73, 2252–2282.
Guidry, M.W., Mackenzie, F.T., 2003. Experimental study of igneous and sedimentary apatite dissolution: control of pH, distance from equilibrium, and temperature on dissolution rates. Geochim. Cosmochim. Acta 67 (16), 2949–2963.
Hartmann, J., Moosdorf, N., Lauerwald, R., Hinderer, M., West, A.J., 2014. Global chemical weathering and associated P-release - the role of lithology, temperature and soil properties. Chem. Geol. 363, 145–163.
Hedley, M.J., Stewart, J.W.B., Chauhan, B., 1982. Changes in inorganic and organic soil phosphorus fractions induced by cultivation practices and by laboratory incubations 1. Soil Sci. Soc. Am. J. 46, 970–976.
Hinsinger, P., 2001. Bioavailability of soil inorganic P in the rhizosphere as affected by root-induced chemical changes: a review. Plant Soil 237, 173–195.
Hou, E., Chen, C., Luo, Y., Zhou, G., Kuang, Y., Zhang, Y., et al., 2018. Effects of climate on soil phosphorus cycle and availability in natural terrestrial ecosystems. Glob. Chang. Biol. 24, 3344–3356.
Hulton, N.R., Purves, R.S., McCulloch, R.D., Sugden, D.E., Bentley, M.J., 2002. The last glacial maximum and deglaciation in southern South America. Quat. Sci. Rev. 21, 233–241.
Ippolito, J.A., Blecker, S.W., Freeman, C.L., McCulley, R.L., Blair, J.M., Kelly, E.F., 2010. Phosphorus biogeochemistry across a precipitation gradient in grasslands of central North America. J. Arid Environ. 74, 954–961.
Jones, D.L., Oburger, E., 2011. Solubilization of phosphorus by soil microorganisms. In: Bünemann, E.K., Oberson, A., Frossard, E. (Eds.), Phosphorus in Action. Springer, Berlin Heidelberg, pp. 169–198.
Lajtha, K., Schlesinger, W.H., 1988. The biogeochemistry of phosphorus cycling and phosphorus availability along a desert soil chronosequence. Ecology 69, 24–39.
Maher, K., 2010. The dependence of chemical weathering rates on fluid residence time. Earth Planet. Sci. Lett. 294, 101–110.
Miller, A.J., Schuur, E.A., Chadwick, O.A., 2001. Redox control of phosphorus pools in Hawaiian montane forest soils. Geoderma 102, 219–237.
Murphy, J., Riley, J.P., 1962. A modified single solution method for the determination of phosphate in natural waters. Anal. Chim. Acta 27, 31–36.
Oeser, R.A., Stroncik, N., Moskwa, L.M., Bernhard, N., Schaller, M., Canessa, R., et al., 2018. Architecture, chemistry, and microbiology of the critical zone along a steep climate gradient in the Chilean Coastal Cordillera. Catena 170, 183–203.
Penuelas, J., Poulter, B., Sardans, J., Ciais, P., Van Der Velde, M., Bopp, L., ... Nardin, E., 2013. Human-induced nitrogen–phosphorus imbalances alter natural and managed ecosystems across the globe. Nat. Commun. 4, 2934.
Porder, S., Vitousek, P.M., Chadwick, O.A., Chamberlain, C.P., Hilley, G.E., 2007. Uplift, erosion, and phosphorus limitation in terrestrial ecosystems. Ecosystems 10, 159–171.
Richardson, S.J., Peltzer, D.A., Allen, R.B., McGlone, M.S., Parfitt, R.L., 2004. Rapid development of phosphorus limitation in temperate rainforest along the Franz Josef soil chronosequence. Oecologia 139, 267–276.
Riebe, C.S., Kirchner, J.W., Finkel, R.C., 2003. Long-term rates of chemical weathering and physical erosion from cosmogenic nuclides and geochemical mass balance. Geochim. Cosmochim. Acta 67, 4411–4427.
Saunders, W.M.H., Williams, E.G., 1955. Observations on the determination of total organic phosphorus in soils. Eur. J. Soil Sci. 6, 254–267.
Schaller, M., Ehlers, T.A., Lang, K.A.H., Schmid, M., Fuentes-Espoz, J.P., 2018. Addressing the contribution of climate and vegetation cover on hillslope denudation, Chilean Coastal Cordillera (26°–38° S). Earth Planet. Sci. Lett. 489, 111–122.
Selmants, P.C., Hart, S.C., 2010. Phosphorus and soil development: does the Walker and Syers model apply to semiarid ecosystems? Ecology 91, 474–484.
Spohn, M., Sierra, C.A., 2018. How long do elements cycle in terrestrial ecosystems? Biogeochemistry 139, 69–83.
Tiessen, H., Moir, J.O., 1993. Characterization of available P by sequential extraction. In: Carter, M.R., Gregorich, E.G. (Eds.), Soil Sampling and Methods of Analysis, second edition. CRC Press, Boca Raton, pp. 5–229.
Trenberth, K.E., Dai, A., Van Der Schrier, G., Jones, P.D., Barichivich, J., Briffa, K.R., Sheffield, J., 2014. Global warming and changes in drought. Nat. Clim. Chang. 4, 17.
Uroz, S., Calvaruso, C., Turpault, M.P., Frey-Klett, P., 2009. Mineral weathering by bacteria: ecology, actors and mechanisms. Trends Microbiol. 17, 378–387.
Vitousek, P.M., Chadwick, O.A., 2013. Pedogenic thresholds and soil process domains in basalt-derived soils. Ecosystems 16, 1379–1395.
Walker, T.W., Adams, A.F.R., 1958. Studies on soil organic matter: I. Influence of phosphorus content of parent materials on accumulations of carbon, nitrogen, sulfur, and organic phosphorus in grassland soils. Soil Sci. 85, 307–318.
Walker, T.W., Syers, J.K., 1976. The fate of phosphorus during pedogenesis. Geoderma 15, 1–19.
Wardle, D.A., Walker, L.R., Bardgett, R.D., 2004. Ecosystem properties and forest decline in contrasting long-term chronosequences. Science 305, 509–513.
Werner, C., Schmid, M., Ehlers, T.A., Fuentes-Espoz, J.P., Steinkamp, J., Forrest, M., ... Hickler, T., 2018. Effect of changing vegetation and precipitation on denudation–part 1: predicted vegetation composition and cover over the last 21 thousand years along the Coastal Cordillera of Chile. Earth Surf. Dyn. 6, 829–858.
West, A.J., Galy, A., Bickle, M., 2005. Tectonic and climatic controls on silicate weathering. Earth Planet. Sci. Lett. 235, 211–228.
Yang, X., Post, W.M., 2011. Phosphorus transformations as a function of pedogenesis: a synthesis of soil phosphorus data using Hedley fractionation method. Biogeosciences 8, 2907–2916.
Zhou, J., Bing, H., Wu, Y., Sun, H., Wang, J., 2018. Weathering of primary mineral phosphate in the early stages of ecosystem development in the Hailuogou Glacier foreland chronosequence. Eur. J. Soil Sci. 69, 450–461.